Role of Nucleotides in Stabilization of the Phospholamban/Cardiac Ca^{2+} Pump Inhibitory Complex Examined by Metal Fluorides *

Zhenhui Chen[‡]

From the Krannert Institute of Cardiology and the Department of Medicine, Indiana University School of Medicine, Indianapolis, IN 46202

*Running title: *Competition between PLB and MFs binding to E2*

[‡]Correspondence should be addressed: Krannert Institute of Cardiology, 1800 N. Capitol Ave., Indianapolis, IN, 46202

Tel.: 317-274-0964 Fax: 317-962-0505 E-mail: zhechen@iu.edu

Keywords: phospholamban, calcium ATPase, metal fluorides, protein cross-linking.

[1]The abbreviations used are: PLB, phospholamban; 2D12, anti-PLB monoclonal antibody; SR, sarcoplasmic reticulum; SERCA, sarco(endo)plasmic reticulum Ca^{2+}-ATPase; SERCA1a or SERCA2a, isoform of Ca^{2+}-ATPase in fast twitch skeletal muscle or cardiac SR, respectively; MOPS, 3-(N-morpholino)propanesulfonic acid; *E*1 or *E*2, high or low Ca^{2+} affinity conformation of Ca^{2+}-ATPase, respectively; *K*, concentration giving half-maximal effect; MFs, metal fluorides; TG, thapsigargin; KMUS (N-[κ-maleimidoundecanoyloxy] sulfosuccinimide ester); bBBr, dibromobimane; Pi, inorganic phosphate; VD , vanadate; WT, wild-type.

Conflict of interest

None

This is the author's manuscript of the article published in final edited form as:
Chen, Z. (2015). Role of nucleotides in stabilization of the phospholamban/cardiac Ca $^{2+}$ pump inhibitory complex examined with use of metal fluorides. FEBS Journal, 282(22), 4402–4414.
http://doi.org/10.1111/febs.13506

ABSTRACT

Phospholamban (PLB) inhibits the activity of cardiac calcium pump (SERCA2a). We previously showed that PLB with engineered Cys-residues only cross-linked to the Ca^{2+}-free, *E*2 intermediate of SERCA2a. The formation of *E*2•PLB prevents Ca^{2+} binding at the high affinity Ca^{2+} binding sites and blocking the enzyme kinetic cycle. Here we further studied synergistic action of PLB and ATP on *E*2 in prevention of forming the phosphorylated *E*2P-like states stabilized by metal fluorides. SERCA2a was co-expressed in insect cell microsomes with PLB mutants of normal or super-inhibitory strength, with cross-linkable mutations at either cytosolic (N30C) or luminal (V49C) sides of PLB. For normal strength PLB mutants, in the absence of nucleotide, metal fluorides totally inhibited both SERCA2a enzyme activity and cross-linking of PLB to SERCA2a at both sites, suggesting that PLB dissociated from SERCA2a in the *E*2P-like states. However, at the same condition, super-inhibitory PLB mutants prevented total enzyme inhibition by metal fluorides. Further, the cross-linking of super-inhibitory PLB to SERCA2a was only partially inhibited by metal fluorides, but was drastically restored upon sequential addition of ATP. These results revealed the equilibrium between *E*2•PLB, *E*2•ATP, or *E*2•ATP•PLB states and *E*2P-like states, suggesting that the synergistic binding of ATP and PLB to SERCA is very strong, sufficient to prevent formation of *E*2 phosphoenzymes, even when stabilized by metal fluorides.

INTRODUCTION

Phospholamban (PLB[1]), a 52 amino acid, single-transmembrane domain protein, inhibits the Ca^{2+}-ATPase (SERCA2a isoform) in cardiac SR [1, 2] by decreasing its apparent affinity for Ca^{2+} ions. Phosphorylation of PLB at Ser^{16} (by cAMP-dependent protein kinase A) or Thr^{17} (by calmodulin kinase II) partially reverses enzyme inhibition, thus increasing SR Ca^{2+} uptake at low ionized Ca^{2+} concentrations [1] and augmenting cardiac contractile forces [1]. The anti-PLB monoclonal antibody 2D12 prevents WT-PLB/SERCA2a heterodimer formation, fully reversing WT-PLB inhibition of SERCA2a [3-5].

SERCA pumps Ca^{2+} into the SR (ER) lumen through a complex catalytic cycle [6-8](Fig. 1). Two Ca^{2+} ions bind to the high Ca^{2+} affinity binding sites at the cytoplasmic face of SR (ER) (*E*1•Ca_2). Autophosphorylation at Asp^{351} and subsequent transition into low Ca^{2+} affinity *E*2 phosphoenzyme release 2 Ca^{2+} into the lumen, before dephosphorylation of *E*2 phosphoenzyme occurs to form the low Ca^{2+} affinity *E*2 dephosphoenzyme [9]. The *E*2 phosphoenzyme intermediates are sensitive to Ca^{2+} and ATP [10], but can be stabilized by various SERCA inhibitors. For example, metal fluorides (MFs) BeF_x, AlF_x, and MgF_x are known to mimic inorganic phosphate and stabilize SERCA1a in the discrete *E*2P-like conformations, specifically the ground *E*2P state, the transition *E*2~P state, and the product *E*2•Pi state, respectively [9-15] (Fig 1). In addition, VD or TG stabilizes SERCA in transition *E*2~P state or the ground *E*2 state, respectively [9]. Recently, 3D crystal structures for several of these conformations were resolved for SERCA1a (See reviews in [6-8]).

We proposed that among the entire catalytic cycle, PLB interacts with a unique *E*2 state of SERCA2a [4, 16-19]. The formation of *E*2•PLB slows the enzyme transition to *E*1, thus competing for Ca^{2+} binding to *E*1, and thereby decreasing the apparent Ca^{2+} affinity of SERCA2a for Ca^{2+}. This model is based on a series of studies, in which we showed that cross-linking of PLB to SERCA2a at both cytoplasmic and transmembrane domains with an array of cross-linkers only occurs in the Ca^{2+} free states, but is completely inhibited by micromolar Ca^{2+} [16, 20-23], Pi [16], TG [16, 17, 20, 22], VD [17], or 2D12 [4]. Thus, PLB does not associate with SERCA2a through the entire catalytic cycle [24], but has to completely dissociate from *E*1, *E*2•TG or *E*2•VD. Consistent with this idea, super-inhibitory PLB mutants were shown to have much higher binding affinity for *E*2, thus super-shifting the Ca^{2+}-dependent ATPase activity [17, 23]. Further, we recently obtained a 3D crystal structure of SERCA1a with bound PLB (*E*2-PLB)[25], which is formed in the Ca^{2+}-free condition in a detergent system that preserves SERCA activity and its interaction with PLB. Although sharing a globally similar structure with the *E*1•Mg state [26, 27], *E*2-PLB has collapsed Ca^{2+} binding sites that are devoid of divalent cations, confirming the cross-linking results and the mutually exclusive binding of PLB and Ca^{2+} to the enzyme.

One of our early findings is that PLB4, the most potent super-shifting PLB mutant, and ATP synergistically stabilize *E*2 that is remarkably resistant to SERCA inhibitors, including TG and VD [16, 17]. However, due to TG interaction with multiple conformations of SERCA, Ca^{2+}-dependent ATPase activity assay is not suitable for further functional characterization. On the other hand, the effect of less potent SERCA inhibitors, MFs, on SERCA2a activity remains largely uninvestigated, with only a few earlier reports, in which PLB was shown not to affect interactions between fluoride and SERCA2a [28, 29].

Here, using insect cell membranes with co-expression of SERCA2a and PLB mutants with increasing inhibitory strength, we evaluated effects of MFs on physical interactions between PLB and SERCA2a at both cytosolic and luminal sides, as well as on functional Ca^{2+}-dependent ATPase activity. Possible mechanism of synergistic PLB and ATP binding to *E*2 is discussed.

RESULTS

Effect of metal fluorides on Ca^{2+}-dependent ATPase activity of cardiac SR membranes — As shown in Fig. 2A, in the absence of both Ca^{2+} and nucleotide, a 10 min pre-incubation with MFs at concentrations reported for saturating inhibition for SERCA1a [9, 10] totally inhibited SERCA2a activity in the canine cardiac SR membranes in the low micromolar Ca^{2+} concentration range, suggesting the irreversible stabilization of the *E*2P-like states by MFs. At greater than 10 μM Ca^{2+} concentrations, samples pre-treated with BeF_x showed some recovery in the Ca^{2+}-dependent ATPase activity (*diamonds*). This ability of Ca^{2+} to restore activity was reported for SERCA1a previously [10] and attributed to the fact that the *E*2•BeF_x state can bind luminal Ca^{2+} at the low Ca^{2+} affinity site, leading to its destabilization at high Ca^{2+} concentrations [30]. Thus, MFs appear to have similar effect to inhibit the activity of both SERCA2a and SERCA1a.

To determine if PLB interferes with MFs inhibition of SERCA2a, we compared the effect of 2D12 on the MFs concentration-dependent inhibition of SERCA2a activity in cardiac SR membranes (Fig. 2B). A higher concentration of MFs is required to inhibit SERCA2a activity in the absence of 2D12 when PLB

is bound. Addition of 2D12 shifted the dose-dependent inhibition curves to the left (compare *open* to *closed* symbols), decreasing K_i values for MFs (Table 2). These results demonstrate for the first time that PLB protects against MFs inhibition of SERCA2a activity.

Identical experiments were also conducted using insect cell membranes co-expressing SERCA2a and PLB. Relative to SERCA2a expressed alone, co-expression of WT-PLB shifted the dose-dependent MFs inhibition of SERCA2a enzyme activity to the right, significantly increasing K_i values (Table 2). Thus, similar to that for native PLB in cardiac SR membranes, co-expression of WT-PLB in insect cells protected against MFs inhibition of SERCA2a activity.

The effect of PLB mutants of different inhibitory strength on metal fluorides inhibition of SERCA2a — To determine if super inhibitory PLB mutants provide better protection, we co-expressed WT-SERCA2a with normal inhibitory strength N30C-PLB, or super-inhibitory strength PLB4 [17] in insect cells. Both PLB mutants contain a Cys mutation at Asn^{30} of PLB in cytoplasmic domain IB, which cross-links highly specifically to Lys^{328} of SERCA2a in the phosphorylation domain [17]. In addition, we also co-expressed V89C-SERCA2a with normal inhibitory strength V49C-PLB, and a new super-inhibitory PLB mutant PLB4C-term, both containing a Cys mutation at Val^{49} of PLB, to study the interactions between the two proteins at the opposite (intra-luminal) face of the SR membrane.

As expected, Fig.3 shows that relative to SERCA2a co-expressed with PLB of normal inhibitory strength (N30C-PLB or V49C-PLB), gain-of-function PLB mutants (PLB4 and PLB4C-term) super-shifted the Ca^{2+}-dependent curves of SERCA2a activity far to the right (*upper panels*, See table 1 for K_{Ca} values). Similar to that occurred in the cardiac SR membranes (Fig. 2A) and insect cell membranes with co-expression of WT-PLB and SERCA2a, saturating concentration of MFs completely inhibited Ca^{2+}-ATPase activity of SERCA2a with co-expression of N30C-PLB or V49C-PLB (*Triangles*). In sharp contrast, in the presence of the same saturating concentration of MFs and absence of nucleotides and Ca^{2+}, PLB4 and PLB4C-term partially restored SERCA2a activity. Specifically, at high μM Ca^{2+} concentrations, SERCA2a co-expressed with PLB4C-term or PLB4 retained about 60-80% of maximal Ca^{2+}-dependent ATPase activity against inhibition by MFs (*Squares*). These results demonstrate that

PLB super-shifters protect against inhibition of SERCA2a even at saturating concentrations of MFs. Cross-linking of PLB to SERCA2a was next examined to see if effects of MFs on PLB binding to SERCA2a and on Ca^{2+}-dependent ATPase activity are correlated.

The effect of metal fluorides on PLB cross-linking to SERCA2a — As shown in Fig. 4A, in the absence of nucleotide and Ca^{2+}, MFs pre-incubation in these samples completely inhibited cross-linking of N30C-PLB to Lys^{328} or V49C-PLB to V89C of SERCA2a, respectively. The identical results were obtained with TG, forming the irreversibly inhibited dead end complex (*E*2•TG)[16, 22]. These results suggest that PLB does not interact with these *E*2P-like states stabilized by MFs at both cytoplasmic and transmembrane domain of PLB.

In contrast, in the presence of MFs, PLB4 and PLB4C-term retained the ability to cross-link to SERCA2a (Fig 4B). Cross-linking was strongest in the presence of MgF_x, and somewhat lower in the presence of AlF_x or BeF_x, which qualitatively correlate well with the PLB super-shifters protection of SERCA2a enzyme activity (Fig. 3). These results demonstrate that these PLB super-shifters remain able to form *E*2•PLB even in the presence of MFs.

Metal fluorides concentration curves on the PLB cross-linking to SERCA2a and the enzyme activity —As shown in Fig. 5, in the absence of Ca^{2+} and nucleotide, MFs inhibited both the cross-linking of N30C-PLB or V49C-PLB to SERCA2a and the Ca^{2+}-dependent ATPase activity in a correlated concentration-dependent manner (*open symbols*)(Table 3). These results suggest that the binding of PLB and MFs to SERCA2a are competitive. Further, dose-dependent inhibition of Ca^{2+}-dependent ATPase activity and cross-linking for PLB4 or PLB4C-term to SERCA2a were also correlated (Fig 5, *red solid symbols*). Importantly, compared to that for the regular inhibitory strength PLB, the MFs dose response curves for Ca^{2+}-dependent ATPase activity and cross-linking of super-inhibitory PLB to SERCA2a were significantly shifted to the right, strongly suggesting that higher PLB binding affinity for SERCA2a increased formation of *E*2•PLB and decreased MFs inhibition of SERCA2a.

Effect of nucleotide ADP or ATP on metal fluorides inhibition of PLB cross-linking to SERCA2a — Although the two assays yielded consistent results, one of the major discrepancies is the use of ATP, which is present in the Ca^{2+}-dependent ATPase assay but absent in the cross-linking assay. Note that nucleotide, ADP or ATP, is known to disrupt the formation of *E*2P by MFs [11] and promotes formation of PLB binding *E*2•Nuc conformation [16, 17, 20, 22]. We thus added ADP or ATP sequentially 10 minutes after samples incubation with MFs, and then measured both cross-linking of PLB to SERCA2a and Ca^{2+}-dependent ATPase activity. In the case for normal inhibitory strength PLB mutants, the Ca^{2+}-dependent ATPase activity assay revealed that MFs totally inhibited enzyme activity in these samples even after sequential addition of ADP or ATP (Fig. 6A, *upper panels*). This is also consistent with results that cross-linking of PLB and SERCA2a was almost completely inhibited (Fig. 6B, *upper panels*). Therefore, normal inhibitory strength PLB does not interact with these *E*2P-like states stabilized by MFs, regardless of ATP or ADP binding to these states [9]. In addition, these results suggest that once formed, these MFs-induced *E*2P-like states were stable, yet different from the *E*2•Nuc, *E*2•PLB, or *E*2•Nuc•PLB state [16, 22]. Thus, formation of the *E*2P-like states by MFs inhibited Ca^{2+}-ATPase activity and at the same time prevented *E*2•Nuc•PLB formation even in the presence of N30C-PLB or V49C-PLB.

In the case for PLB super-shifters (Fig. 6A & B, *lower panels*), when ADP or ATP was sequentially added after samples incubation with MFs, PLB4 and PLB4C-term preserved 60-80% and 50-70% of SERCA2a activity, respectively. Remarkably though, in contrast to that for the effect of N30C-PLB or V49C-PLB, sequential addition of ADP or ATP after samples incubation with MFs significantly increased percentage of cross-linking of SERCA2a to PLB4 or PLB4C-term (Fig. 6B, *lower panels, +ADP or +ATP vs -Nuc*). After sequential addition of ADP or ATP, the cross-linking of SERCA2a to PLB4 or PLB4C-term in MFs significantly increased from 40-65% to 70-95% or from 30-45% to 60-92% of the controls, respectively. For MgF_x, cross-linking of SERCA2a to PLB4 or PLB4C-term was reached above 90% of the maximal intensity after sequential addition of ADP or ATP. Note that although very faint, addition of ADP or ATP weakly restored cross-linking of normal inhibitory strength V49C-PLB to V89C-SERCA2a in the presence of MgF_x (Fig. 5B,). These results suggest that the binding of PLB super

shifters, which has profound long-range conformational effects on both the cytoplasmic domains and the transmembrane domain previously shown to prevent *E*1•Ca_2 [17], synergistically promotes nucleotide binding and formation of *E*2•Nuc•PLB, giving ATP the ability to recover SERCA2a previously inhibited by MFs.

ATP concentration curves on the PLB cross-linking to SERCA2a — We observed that in conditions when either nucleotide and MFs are simultaneously added, or nucleotide first and then MFs are sequentially added, MFs inhibition of both SERCA2a enzyme activity and cross-linking to PLB was drastically reduced (data not shown), showing that ADP or ATP protects SERCA2a from MFs inhibition in these conditions as it was previously demonstrated for SERCA1a [11]. We examined ATP dependency in stimulation of cross-linking of PLB to SERCA2a in these samples with simultaneous incubation of ATP and MFs. The presence of MFs significantly shifted the curves of ATP stimulation of PLB cross-linking to SERCA2a to the right (Fig. 7), yielding a 5-10 fold increase in the K_{ATP} values (Table 4). These results suggest MFs reduced the amount of *E*2•ATP•PLB complex and decreased the apparent ATP affinity for SERCA2a in these conditions. Moreover, compared to that occurred for N30C-PLB or V49C-PLB, in the presence of MFs, ATP stimulation curves of cross-linking for PLB4 and PLB4C-term to SERCA2a were all significantly shifted to the left (Fig. 7), yielding much smaller K_{ATP} values (Table 4). In the case for the strongest super-shifting mutant PLB4, MFs only marginally shifted the curves, suggesting that ATP may not be necessary for *E*2•PLB4 to resist MFs binding to the pump. These results suggest that increased inhibitory strength of PLB and ATP synergistically promotes formation of *E*2•ATP•PLB, thus preventing the formation of *E*2P-like states in the presence of MFs.

DISCUSSION

In this study, using cardiac SR membranes and insect cell microsomes co-expressing PLB and SERCA2a, we biochemically examined the effect of MFs on the molecular interactions between SERCA2a and PLB, in the presence and absence of ATP. Our results demonstrate that synergistic

binding of PLB and ATP to *E*2 protects against enzyme inhibition and prevents formation of *E*2•Pi, *E*2~P, or *E*2P states, even when stabilized by MFs.

Reversible binding of PLB to SERCA2a — In addition to noted difference to *E*1 [25], the structure of *E*2-PLB is also different from any other *E*2 structures crystallized in the presence of SERCA inhibitors, e.g, MFs or TG [7, 8]. In particular, in *E*2-PLB structure, the global rearrangement of M2, M4, M6 and M9 forms a groove that fits PLB binding [25]. However, when SERCA1a is stabilized with MFs, the groove becomes almost flat, thus unable for PLB to dock. These structural differences are compatible with the present study, in which we showed that the inhibition of both SERCA2a activity and PLB cross-linking to SERCA2a at both faces of SR membranes are highly correlated in a MFs concentration-dependent manner (or amount of stabilized *E*2P-like states) (Fig. 5), and is influenced by the inhibitory strength of PLB. These results lead to the conclusion that when SERCA2a is stabilized in *E*2P-like states by MFs, the entire PLB molecule must completely dissociate from the enzyme (Fig.4). Therefore, as SERCA2a transits from *E*2P to *E*2 and then to *E*1•Ca_2, PLB must be able to bind specifically to *E*2 and then dissociate from *E*1•Ca_2.

*E*2•*ATP and dephosphorylation process for E2P* — Early biochemical studies reveal that the SERCA reaction cycle consists of at least 5 distinct low Ca^{2+} affinity *E*2 states, including *E*2•ATP, *E*2, *E*2•Pi, *E*2~P, or *E*2P (Fig. 1). As recently shown by Clausen *et al* [9], ATP is capable to bind at the modulatory site to all these *E*2P states, but with different affinity. These authors suggest that the ATP stabilization of the transition and product states, which have relative high affinity for ATP, is involved in *E*2 phosphoenzyme dephosphorylation process [9]. However, we showed that the apparent ATP affinity, tested by ATP stimulation of PLB cross-linking to SERCA2a in the presence of MFs (Fig. 7), remains similar for all these *E*2P-like states. Further, we showed that ADP acts similarly to ATP in protection of enzyme activity and formation of *E*2•ADP•PLB. Since it is well established that these *E*2P-like states are insensitive to ADP [10], binding of ATP to these *E*2P-like states appears not to be the sole reason for the acceleration of dephosphorylation of *E*2P, at least for SERCA2a. Instead, among these *E*2 states for

SERCA2a, *E*2•ATP appears to be a more thermodynamically favorable state that is involved in promoting stimulation of H^+/Ca^{2+} cation exchange and enzyme transition into *E*1•Ca [31], as well as dephosphorylation of *E*2 phosphoenzyme.

An advantage of our approach is the use of 2D12, which specifically removes PLB interaction with SERCA2a [3-5], thus unmasking the protective effect of PLB. Hawkins *et al* showed that phosphorylation of PLB did not alter the sensitivity of SERCA2a to inhibition by fluorides [29]. However, phosphorylation of PLB introduced ATP, which itself affects fluorides inhibition. Another advantage of our approach using PLB as a specific probe is that we correlate the Ca^{2+}-dependent ATPase activity assay (requiring addition of ATP, Ca^{2+}, and Ca^{2+} ionophore A23187), with the cross-linking of PLB to SERCA2a (occurring in the Ca^{2+}-free condition), making it possible to test directly the equilibrium between *E*2•ATP, *E*2, and *E*2P-like states. We showed that ATP and PLB act independently and synergistically against formation of *E*2P-like states. Thus, the mechanism by which nucleotide [11, 15] or PLB protects SERCA inhibition by MFs from can be attributed to the promotion of *E*2•Nuc or *E*2•PLB formation. Further, although PLB binds to both *E*2 with and without ATP binding at the modulatory site, *E*2•ATP, an intimate part of the SERCA kinetic cycle, might be the physiological conformation that favors PLB binding and forming a more stable complex. Finally, based on the similarities in biochemical properties between *E*2•ATP and *E*2•PLB, we propose that *E*2•PLB or *E*2•ATP have similar structural motifs (e.g., favoring formation of both a binding grove for PLB at the transmembrane domain and a binding pocket for ATP in the N-domain), allowing PLB and ATP to interact synergistically to stabilize *E*2•PLB•ATP, which most strongly competes against binding of other inhibitors (e.g., MFs [11], TG [17, 32], VD [17, 33]). This hypothesis can ultimately be proved by resolving 3D crystal structure of these conformations, particularly for SERCA2a.

EXPERIMENTAL PROCEDURES

Preparation of canine cardiac SR membranes— The study protocol was approved by the Indiana University Institutional Animal Use and Care Committee and conforms to the Guide for the Care and Use of Laboratory Animals. Cardiac microsomes enriched in SR (45,000 x *g* pellets) were prepared from the left ventricles of dog hearts as previously described [34]. There is a roughly 1:1 molar stoichiometry between PLB and SERCA2a in these SR membranes [19, 35].

Mutagenesis and Baculovirus Production—Mutagenesis of canine SERCA2a (V89C-SERCA2a) and PLB cDNAs was conducted directly in the transfection vector pVL1393 using the QuickChange™ XL-Gold system (Stratagene) [16, 17, 22]. N30C-PLB and V49C-PLB was made on the Cys-less PLB background, which is fully functional, with Cys residues 36, 41, and 46 changed to Ala. PLB4 is a quadruple (N27A, N30C, L37A, V49G) mutant on WT-PLB background [17]. PLB4C-term has mutations at N27A, N30A, L37A, and V49C on WT-PLB background. All mutated cDNAs were confirmed by DNA sequencing of the plasmid vectors. Baculoviruses encoding mutated proteins were generated with BaculoGold™ (Pharmingen) linearized baculovirus DNA [16, 17, 22].

Protein Expression — Co-expression of SERCA2a and PLB proteins in Sf21 insect cells was achieved by baculoviruse infection and was quantified with the monoclonal antibodies 2A7-A1 and 2D12, respectively [4, 36]. Microsomes were harvested 60 h after infection and stored frozen in small aliquots at -40 ºC at a protein concentration of 6-10 mg/ml in 0.25 M sucrose, 10 mM MOPS (pH 7.0). Protein concentration was measured by the Lowry assay. Membranes co-expressing PLB and SERCA2a at a molar ratio in a range of 1:1 to 4:1 were used for current studies. All PLB mutants used in this study were predominantly monomers on 15% SDS-PAGE as noted previously [16, 17, 20, 22].

Formation of E2P-like states by MFs— microsomes were incubated for 10 min at room temperature in buffer A (40 mM MOPS (pH 7.0) and 75 mM KCl) with 1 mM EGTA and MFs. MFs were used to stabilize various intermediate forms occurring during the *E*2P dephosphorylation reaction sequence. The MgF_x product state was formed in 5mM $MgCl_2$ and 5mM NaF. The AlF_x transition state was formed in 0.2mM $MgCl_2$, 2mM NaF, 0.5 mM $AlCl_3$. The BeF_x ground state was formed in 0.2 mM $MgCl_2$, 2mM

NaF, 0.1 mM $BeSO_4$. These conditions are used to produce saturating inhibition of SERCA1a [9, 10]. In some experiments, diluted MFs were used as indicated.

Cross-linking— The heterobifunctional thiol-to-amine cross-linking reagent, KMUS (Pierce), or homobifunctional thiol-to-thiol cross-linking reagent, bBBr, was used to cross-link of residue N30C of PLB to Lys^{328} of SERCA2a, or V49C of PLB to V89C of SERCA2a, respectively, as described previously [16, 22]. Prior to cross-liking, 11 µg of microsomal protein was incubated for 10 min at room temperature with MFs in 12 µl of buffer A and 1 mM EGTA. In some experiments, 3 mM ADP or ATP was included in the buffer before, together, or 10 minute after incubation with MFs as indicated. Cross-linking reactions were started by adding 0.75 µl of KMUS or bBBr from 1.6 mM stock solutions in DMSO (0.1 mM final cross-linker concentrations), and terminated by adding 7.5 µl of 15% SDS sample buffer containing 100 mM dithiothreitol. Cross-linking reactions time was 10 min for KMUS or 1hr for bBBr. Samples were then subjected to SDS-PAGE followed by immunoblotting with anti-PLB monoclonal antibody, 2D12, to detect PLB cross-linked to SERCA2a. Antibody visualization was routinely with ^{125}I-protein A followed by phosphorimager quantification (BioRad personal Fx). Data analysis was done with Origin (Microcal). In some experiments, concentrations of ATP or MFs were varied, as indicated. TG was added from stock solutions in ethanol.

Ca^{2+}-ATPase Activity Assay— Ca^{2+}-dependent ATPase activities of microsomes were measured using an enzyme-coupled spectrophotometric assay [18, 23]. The rate of NADH decay was measured at 340 nm in a SPECTRAmax® PLUS (Molecular Devices) microplate spectrophotometer at 37 °C. Assay buffer contains buffer A, supplemented with 3mM $MgCl_2$, 5 mM NaN_3, 3 µg/ml of the Ca^{2+} ionophore, A23187, 3 mM ATP and Ca^{2+}/EGTA buffer. The final concentration of EGTA was fixed at 1 mM, and ionized Ca^{2+} concentrations were set by adding $CaCl_2$ from 0 to 1.25 mM. For assay at a full range of Ca^{2+} concentration, 70 µg membranes was incubated in 40 µl of buffer A, 1mM EGTA, and MFs as described in the above section. Some membranes were pretreated with 2D12 to dissociate PLB [4]. In some experiments, 3 mM ADP or ATP was included in the buffer, or added after incubation with MFs as indicated. After incubation, samples were diluted to 280µl with buffer A (final EGTA concentration was

0.25mM). Assay was started by adding 20µl (5µg) protein to 130 µl assay buffer in each well. All ATPase activities reported are Ca^{2+}-dependent.

References

1. Simmerman, H. K. & Jones, L. R. (1998) Phospholamban: protein structure, mechanism of action, and role in cardiac function, *Physiol Rev.* **78**, 921-47.
2. Kranias, E. G. & Hajjar, R. J. (2012) Modulation of cardiac contractility by the phospholamban/SERCA2a regulatome, *Circ Res.* **110**, 1646-60.
3. Sham, J. S., Jones, L. R. & Morad, M. (1991) Phospholamban mediates the beta-adrenergic-enhanced Ca^{2+} uptake in mammalian ventricular myocytes, *Am J Physiol.* **261**, H1344-9.
4. Chen, Z., Akin, B. L. & Jones, L. R. (2007) Mechanism of reversal of phospholamban inhibition of the cardiac Ca^{2+}-ATPase by protein kinase A and by anti-phospholamban monoclonal antibody 2D12, *J Biol Chem.* **282**, 20968-76.
5. Chan, Y. H., Tsai, W. C., Song, Z., Ko, C. Y., Qu, Z., Weiss, J. N., Lin, S. F., Chen, P. S., Jones, L. R. & Chen, Z. (2015) Acute reversal of phospholamban inhibition facilitates the rhythmic whole-cell propagating calcium waves in isolated ventricular myocytes, *J Mol Cell Cardiol.* **80C**, 126-135.
6. Stokes, D. L. & Green, N. M. (2003) Structure and function of the calcium pump, *Annu Rev Biophys Biomol Struct.* **32**, 445-68.
7. Toyoshima, C. (2008) Structural aspects of ion pumping by Ca^{2+}-ATPase of sarcoplasmic reticulum, *Arch Biochem Biophys.* **476**, 3-11.
8. Bublitz, M., Musgaard, M., Poulsen, H., Thogersen, L., Olesen, C., Schiott, B., Morth, J. P., Moller, J. V. & Nissen, P. (2013) Ion pathways in the sarcoplasmic reticulum Ca^{2+}-ATPase, *J Biol Chem.* **288**, 10759-65.
9. Clausen, J. D., McIntosh, D. B., Woolley, D. G. & Andersen, J. P. (2011) Modulatory ATP binding affinity in intermediate states of E2P dephosphorylation of sarcoplasmic reticulum Ca^{2+}-ATPase, *J Biol Chem.* **286**, 11792-802.
10. Danko, S., Yamasaki, K., Daiho, T. & Suzuki, H. (2004) Distinct natures of beryllium fluoride-bound, aluminum fluoride-bound, and magnesium fluoride-bound stable analogues of an ADP-insensitive phosphoenzyme intermediate of sarcoplasmic reticulum Ca^{2+}-ATPase: changes in catalytic and transport sites during phosphoenzyme hydrolysis, *J Biol Chem.* **279**, 14991-8.
11. Murphy, A. J. & Coll, R. J. (1992) Fluoride is a slow, tight-binding inhibitor of the calcium ATPase of sarcoplasmic reticulum, *J Biol Chem.* **267**, 5229-35.
12. Murphy, A. J. & Coll, R. J. (1992) Fluoride binding to the calcium ATPase of sarcoplasmic reticulum converts its transport sites to a low affinity, lumen-facing form, *J Biol Chem.* **267**, 16990-4.
13. Coll, R. J. & Murphy, A. J. (1992) Fluoride-inhibited calcium ATPase of sarcoplasmic reticulum. Magnesium and fluoride stoichiometry, *J Biol Chem.* **267**, 21584-7.
14. Troullier, A., Girardet, J. L. & Dupont, Y. (1992) Fluoroaluminate complexes are bifunctional analogues of phosphate in sarcoplasmic reticulum Ca^{2+}-ATPase, *J Biol Chem.* **267**, 22821-9.
15. Murphy, A. J. & Coll, R. J. (1993) Formation of a stable inactive complex of the sarcoplasmic reticulum calcium ATPase with magnesium, beryllium, and fluoride, *J Biol Chem.* **268**, 23307-10.
16. Chen, Z., Akin, B. L., Stokes, D. L. & Jones, L. R. (2006) Cross-linking of C-terminal residues of phospholamban to the Ca^{2+} pump of cardiac sarcoplasmic reticulum to probe spatial and functional interactions within the transmembrane domain, *J Biol Chem.* **281**, 14163-72.
17. Akin, B. L., Chen, Z. & Jones, L. R. (2010) Superinhibitory phospholamban mutants compete with Ca^{2+} for binding to SERCA2a by stabilizing a unique nucleotide-dependent conformational state, *J Biol Chem.* **285**, 28540-52.
18. Chen, Z. (2011) A phospholamban-tethered cardiac Ca^{2+} pump reveals stoichiometry and dynamic interactions between the two proteins, *Biochem J.* **439**, 313-9.

19. Akin, B. L. & Jones, L. R. (2012) Characterizing phospholamban to sarco(endo)plasmic reticulum Ca^{2+}-ATPase 2a (SERCA2a) protein binding interactions in human cardiac sarcoplasmic reticulum vesicles using chemical cross-linking, *J Biol Chem.* **287**, 7582-93.
20. Jones, L. R., Cornea, R. L. & Chen, Z. (2002) Close proximity between residue 30 of phospholamban and cysteine 318 of the cardiac Ca^{2+} pump revealed by intermolecular thiol cross-linking, *J Biol Chem.* **277**, 28319-29.
21. Toyoshima, C., Asahi, M., Sugita, Y., Khanna, R., Tsuda, T. & MacLennan, D. H. (2003) Modeling of the inhibitory interaction of phospholamban with the Ca^{2+} ATPase, *Proc Natl Acad Sci U S A.* **100**, 467-72.
22. Chen, Z., Stokes, D. L., Rice, W. J. & Jones, L. R. (2003) Spatial and Dynamic Interactions between Phospholamban and the Canine Cardiac Ca^{2+} Pump Revealed with Use of Heterobifunctional Cross-linking Agents, *J Biol Chem.* **278**, 48348-56.
23. Chen, Z. (2014) Competitive displacement of wild-type phospholamban from the Ca-free cardiac calcium pump by phospholamban mutants with different binding affinities, *J Mol Cell Cardiol.* **76c**, 130-137.
24. Karim, C. B., Zhang, Z., Howard, E. C., Torgersen, K. D. & Thomas, D. D. (2006) Phosphorylation-dependent conformational switch in spin-labeled phospholamban bound to SERCA, *J Mol Biol.* **358**, 1032-40.
25. Akin, B. L., Hurley, T. D., Chen, Z. & Jones, L. R. (2013) The structural basis for phospholamban inhibition of the calcium pump in sarcoplasmic reticulum, *J Biol Chem.* **288**, 30181-91.
26. Toyoshima, C., Iwasawa, S., Ogawa, H., Hirata, A., Tsueda, J. & Inesi, G. (2013) Crystal structures of the calcium pump and sarcolipin in the Mg^{2+}-bound E1 state, *Nature.* **495**, 260-4.
27. Winther, A. M., Bublitz, M., Karlsen, J. L., Moller, J. V., Hansen, J. B., Nissen, P. & Buch-Pedersen, M. J. (2013) The sarcolipin-bound calcium pump stabilizes calcium sites exposed to the cytoplasm, *Nature.* **495**, 265-9.
28. Narayanan, N., Su, N. & Bedard, P. (1991) Inhibitory and stimulatory effects of fluoride on the calcium pump of cardiac sarcoplasmic reticulum, *Biochim Biophys Acta.* **1070**, 83-91.
29. Hawkins, C., Xu, A. & Narayanan, N. (1994) Comparison of the effects of fluoride on the calcium pumps of cardiac and fast skeletal muscle sarcoplasmic reticulum: evidence for tissue-specific qualitative difference in calcium-induced pump conformation, *Biochim Biophys Acta.* **1191**, 231-43.
30. Picard, M., Toyoshima, C. & Champeil, P. (2006) Effects of inhibitors on luminal opening of Ca^{2+} binding sites in an E2P-like complex of sarcoplasmic reticulum Ca^{2+}-ATPase with Be^{2+}-fluoride, *J Biol Chem.* **281**, 3360-9.
31. Jensen, A. M., Sorensen, T. L., Olesen, C., Moller, J. V. & Nissen, P. (2006) Modulatory and catalytic modes of ATP binding by the calcium pump, *EMBO J.* **25**, 2305-14.
32. DeJesus, F., Girardet, J. L. & Dupont, Y. (1993) Characterisation of ATP binding inhibition to the sarcoplasmic reticulum Ca^{2+}-ATPase by thapsigargin, *FEBS Lett.* **332**, 229-32.
33. Waggoner, J. R., Huffman, J., Froehlich, J. P. & Mahaney, J. E. (2007) Phospholamban inhibits Ca-ATPase conformational changes involving the E2 intermediate, *Biochemistry.* **46**, 1999-2009.
34. Jones, L. R. & Cala, S. E. (1981) Biochemical evidence for functional heterogeneity of cardiac sarcoplasmic reticulum vesicles, *J Biol Chem.* **256**, 11809-18.
35. Marcelle Stucky, Z. C., Brandy Akin, Larry R. Jones (2013) One to one molar stoichiometry between phospholamban (PLB) and sarco(endo)plasmic reticulum Ca^{2+}-ATPase 2a (SERCA2a) in human and canine cardiac sarcoplasmic reticulum (SR) vesicles. , *Biophys J.* **abstract issue**.
36. Autry, J. M. & Jones, L. R. (1997) Functional Co-expression of the canine cardiac Ca^{2+} pump and phospholamban in Spodoptera frugiperda (Sf21) cells reveals new insights on ATPase regulation, *J Biol Chem.* **272**, 15872-80.

Acknowledgements—We thank Jin Guo for technical assistance.

FOOTNOTES

* This work is supported by the Indiana University Health-Indiana University School of Medicine Strategic Research Initiative and the Dr. Charles Fisch Cardiovascular Research Award endowed by Dr. Suzanne B. Knoebel of the Krannert Institute of Cardiology.

Table 1. K_{Ca} values for Ca^{2+} activation of Ca^{2+}-ATPase activity.

SERCA2a was expressed alone or co-expressed with PLB in insect cell microsomes. Ca^{2+}-ATPase activities were then measured as indicated in Figs. 2, and 3. Maximal Ca^{2+}-ATPase activities ranged between 10 and 15 µmol of ATP hydrolyzed/mg of protein/h for insect cell microsomes co-expressing PLB and SERCA2a [17]. All K_{Ca} values are expressed in units of µM. Results are the means ± S.E. from 3-6 determinations.

	K_{Ca} values	
proteins	Control	2D12
	µM	
Cardiac SR	0.30 ± 0.02	0.13 ± 0.01
WT-SERCA2a	0.15 ± 0.01	0.17 ± 0.04
+WT-PLB	0.35 ± 0.03	0.22 ± 0.02
+ N30C	0.36 ± 0.03	0.22 ± 0.01
+ PLB4	1.48 ± 0.18	0.59 ± 0.07
V89C-SERCA2a	0.14 ± 0.01	0.16 ± 0.02
+ V49C	0.39 ± 0.02	0.23 ± 0.02
+ PLB4C	0.89 ± 0.08	0.36 ± 0.02

Table 2. K_i values for MFs inhibition of Ca^{2+}-ATPase activity.

SERCA2a was expressed alone or co-expressed with PLB in insect cell microsomes. Ca^{2+}-ATPase activities were then measured as indicated in Figs. 2 and 5. All K_i values are expressed as concentrations for 50% inhibition of maximal Ca^{2+}-ATPase activity obtained in the absence of MFs (see Experimental procedures). Results are the means ± S.E. from 3-6 determinations.

	K_i values		
proteins	MgF_x	AlF_x	BeF_x
		µM	
Cardiac SR	2500 ± 50	120 ± 10	35 ± 1
+ 2D12	1850 ± 140	80 ± 11	26 ± 2
WT-SERCA2a	2010 ± 200	115 ±15	18 ± 2
+ WT-PLB	2900 ± 250	170 ± 10	26 ± 3
+ 2D12	2300 ± 150	120 ± 10	17 ± 2

Table 3. K_i values for MFs inhibition of Ca^{2+}-ATPase activity and cross-linking of PLB to SERCA2a.

SERCA2a was co-expressed with PLB in insect cell microsomes. Ca^{2+}-ATPase activities and cross-linking to PLB were then measured as indicated in Fig. 5. All K_i values are expressed as concentrations for 50% inhibition of maximal activity obtained in the absence of MFs (see Experimental procedures). Results are the means ± S.E. from 3-6 determinations.

	K_i values					
	Ca^{2+}-ATPase Activity			Cross-linking		
proteins	MgF_x	AlF_x	BeF_x	MgF_x	AlF_x	BeF_x
	μM					
WT-SERCA2a + N30C	3100 ± 300	145 ± 15	23 ± 2	1400 ± 150	180 ± 15	14 ± 1
V89C-SERCA + V49C	3650 ± 250	165 ± 30	26 ± 3	1700 ± 150	135 ± 10	11 ± 1

Table 4. K_{ATP} values for ATP stimulation of cross-linking of PLB to SERCA2a.

SERCA2a was expressed alone or co-expressed with PLB in insect cell microsomes. ATP effects on cross-linking to PLB were then measured as indicated in Fig. 7. All K_{ATP} values are expressed as concentrations for 50% stimulation of maximal activity obtained in 3 mM ATP. Results are the means ± S.E. from 3-6 determinations. N.D., not determinable.

	K_{ATP} values			
proteins	Control	MgF_x	AlF_x	BeF_x
			μM	
WT-SERCA2a				
+ N30C	7.8 ± 0.4	68.0 ± 19.0	68.5 ± 4.8	91.3 ± 10.2
+ PLB4	16.5 ± 9.9	7.4 ± 2.5	17.3 ± 2.0	8.9 ± 1.6
V89C-SERCA2a				
+ V49C	N.D.	42.3 ± 4.1	105.8 ± 25.6	68.0 ± 11.0
+ PLB4C-term	N.D.	34.7 ± 7.7	30.6 ± 8.6	37.1 ± 7.0

FIGURE LEGENDS

FIGURE 1. **Reaction cycle of SERCA.**

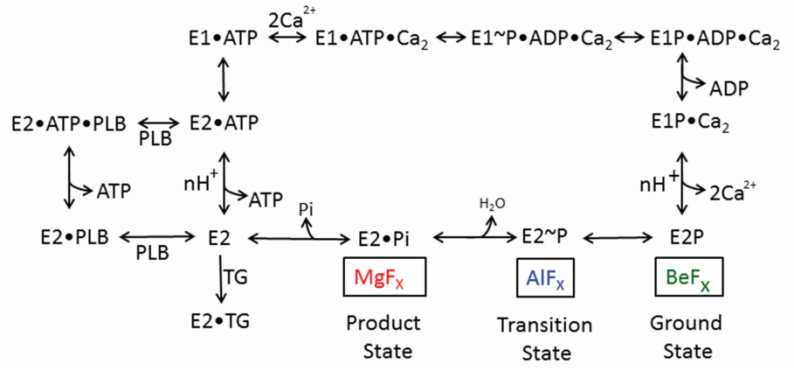

FIGURE 2. **MFs inhibition of Ca^{2+}-dependent ATPase activity of cardiac SR membranes.** Canine cardiac SR membranes were first pre-incubated with (*open symbols*) or without (*solid symbols*) the anti-PLB monoclonal antibody 2D12, and then incubated 10 min in the absence (*Con, squares*) or presence of MgF_x (*circles*), AlF_x(*triangles*), or BeF_x (*diamonds*). Incubations were in the absence of both Ca^{2+} and nucleotide. A. Ca^{2+}-dependent ATPase activity was determined at saturating inhibition concentration of MFs. Similar results were obtained in at least 3 experiments. B. MFs dose-dependent inhibition of Ca^{2+}-dependent ATPase activity. Plot was normalized Ca^{2+}-dependent ATPase activity based on at least 3 experiments for each condition (see text for concentrations). Ca^{2+}-dependent ATPase activity was measured at 0.8 mM Ca^{2+} and 1 mM EGTA. The percent of maximal activity (determined in the absence of MFs) was calculated at each MFs concentration. See Table 2 for K_i values.

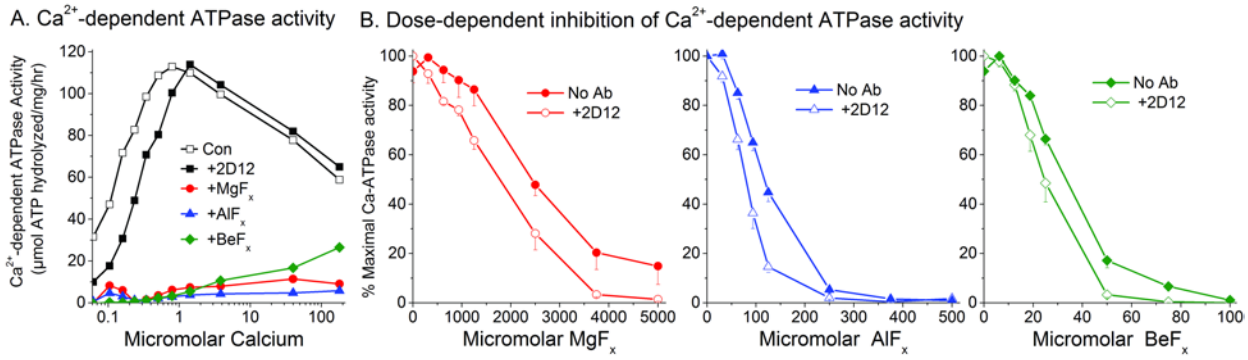

FIGURE 3. **MFs inhibition of Ca^{2+}-ATPase Activities of SERCA2a co-expressed with normal or super-inhibitory PLB mutants.** WT-SERCA2a was expressed alone or co-expressed with N30C-PLB, or PLB4 (*left panels*), and V89C-SERCA2a was expressed alone, or co-expressed with V49C-PLB, or PLB4C-term (*right panels*) in insect cell microsomes as indicated. Ca^{2+}-dependent ATPase activity was determined 10 min after pre-incubation in the absence (*Con*) or in the presence of MgF_x, AlF_x, or BeF_x. Pre-incubation was in the absence of both Ca^{2+} and nucleotide. Maximal Ca^{2+}-ATPase activities ranged between 10 and 15 μmol of ATP hydrolyzed /mg of protein/h for insect cell microsomes co-expressing PLB and SERCA2a. The percent of maximal activity (determined in the absence of MFs) was calculated at each Ca^{2+} concentration for each PLB mutant. See Table 1 for K_{Ca} values.

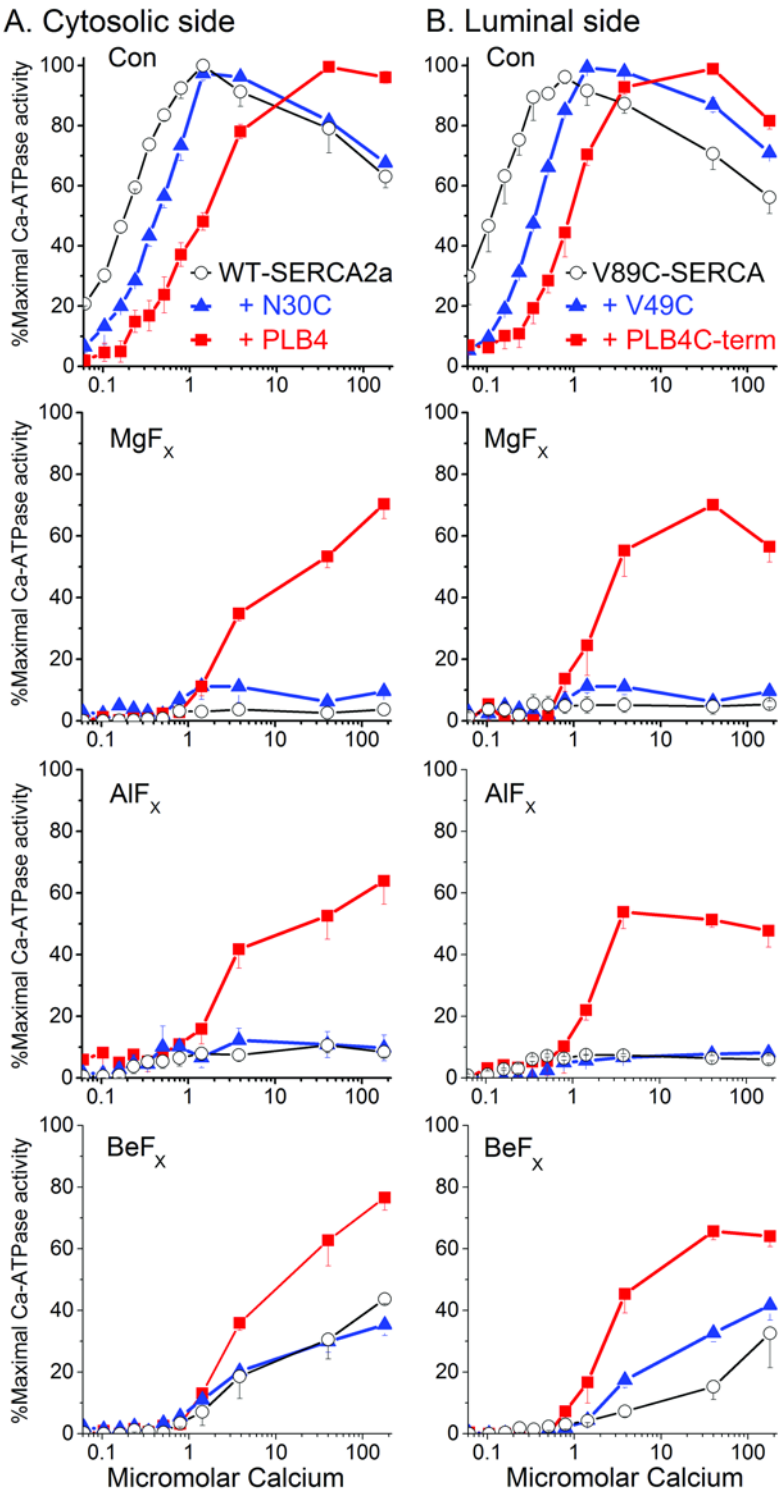
A. Cytosolic side
B. Luminal side
Con
WT-SERCA2a
+ N30C
+ PLB4
V89C-SERCA
+ V49C
+ PLB4C-term
MgFx
AlFx
BeFx
%Maximal Ca-ATPase activity
Micromolar Calcium

FIGURE 4. **MFs inhibition of cross-linking of normal or super-inhibitory strength PLB mutants to SERCA2a.** WT-SERCA2a was co-expressed with N30C-PLB, or PLB4 (*left panels*) and V89C-SERCA2a was co-expressed with V49C-PLB, or PLB4C-term (*right panels*) in insect cell microsomes as indicated. Membranes were incubated in 1mM EGTA in the absence (*Con*) and presence of MgF_x, AlF_x, or BeF_x, before cross-linking reaction as indicated. Reactions were in the absence of nucleotides. N30C-PLB or PLB4 was cross-linked to Lys^{328} of SERCA2a for 10 min using KMUS while V49C-PLB or PLB4C-term was cross-linked to V89C-SERCA2a for 60 min using bBBr in buffer containing 40 mM MOPS (pH 7.0), 3.2 mM $MgCl_2$, 75 mM KCl, (see EXPERIMENTAL PROCEDURES). Reactions were stopped by adding SDS plus dithiothreitol, then samples were subjected to SDS-PAGE followed by immunoblotting with anti-PLB antibody, 2D12, followed by ^{125}I-protein A. *PLB/SER*, PLB cross-linked to SERCA2a; *PLB_1*, PLB monomers. For economy of space, only PLB cross-linked to SERCA2a is displayed in *B*.

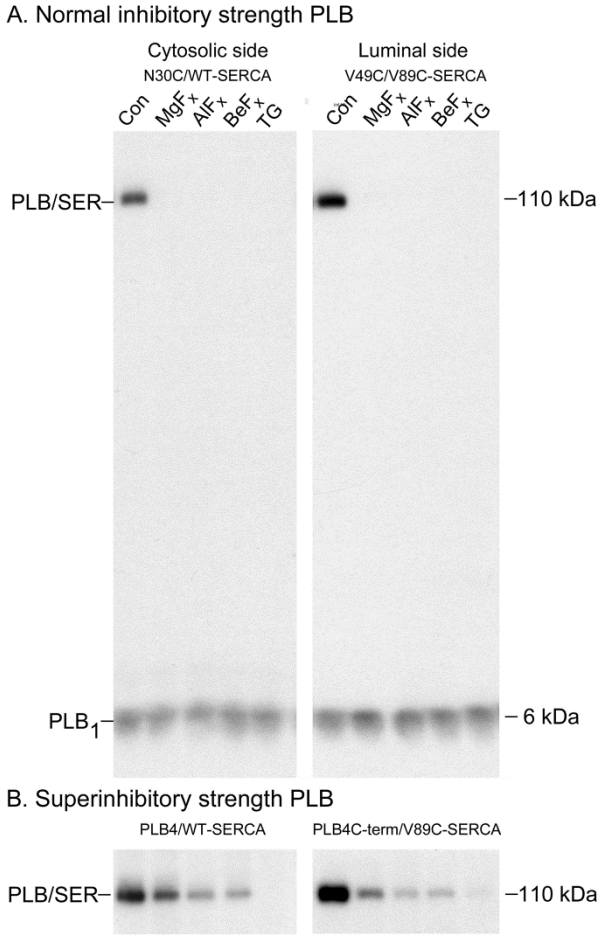

FIGURE 5. **MFs dose response curve for inhibition of SERCA2a activity and PLB to SERCA2a cross-linking.** SERCA2a was co-expressed with PLB mutants in insect cell microsomes and cross-linked as described in the legend to Fig. 4. A. Plot shows the Ca^{2+}-dependent ATPase activity determined 10 min after pre-incubation in the absence both Ca^{2+} and nucleotide and in the presence of a series concentrations of MgF_x (*circles*), AlF_x(*triangles*), or BeF_x (*diamonds*). To obtain maximal Ca^{2+}-dependent ATPase activity, assays were performed at 0.8 mM Ca^{2+} and 1 mM EGTA for SERCA2a co-expressed with N30C-PLB and V49C-PLB, at 1.25 mM Ca^{2+} and 1 mM EGTA for SERCA2a co-expressed with PLB4, or at 1.1 mM Ca^{2+} and 1 mM EGTA for V89C-SERCA2a co-expressed with PLB4C-term. B. Dose dependent inhibition of cross-linking of PLB to SERCA2a. *Upper panels* show representative immunoblots of cross-linking for each PLB mutant to SERCA2a after 10 min pre-incubation in the absence of both Ca^{2+} and nucleotide, and in the presence of a series concentrations of MgF_x, AlF_x, or BeF_x. *Lower panels* plots MFs inhibition of cross-linking for each mutant on a percentage basis (n = 4- 6 for each mutant). The percent of maximal activity (determined in the absence of MFs) was calculated at each MFs concentration for each PLB mutant. See Table 3 for K_i values.

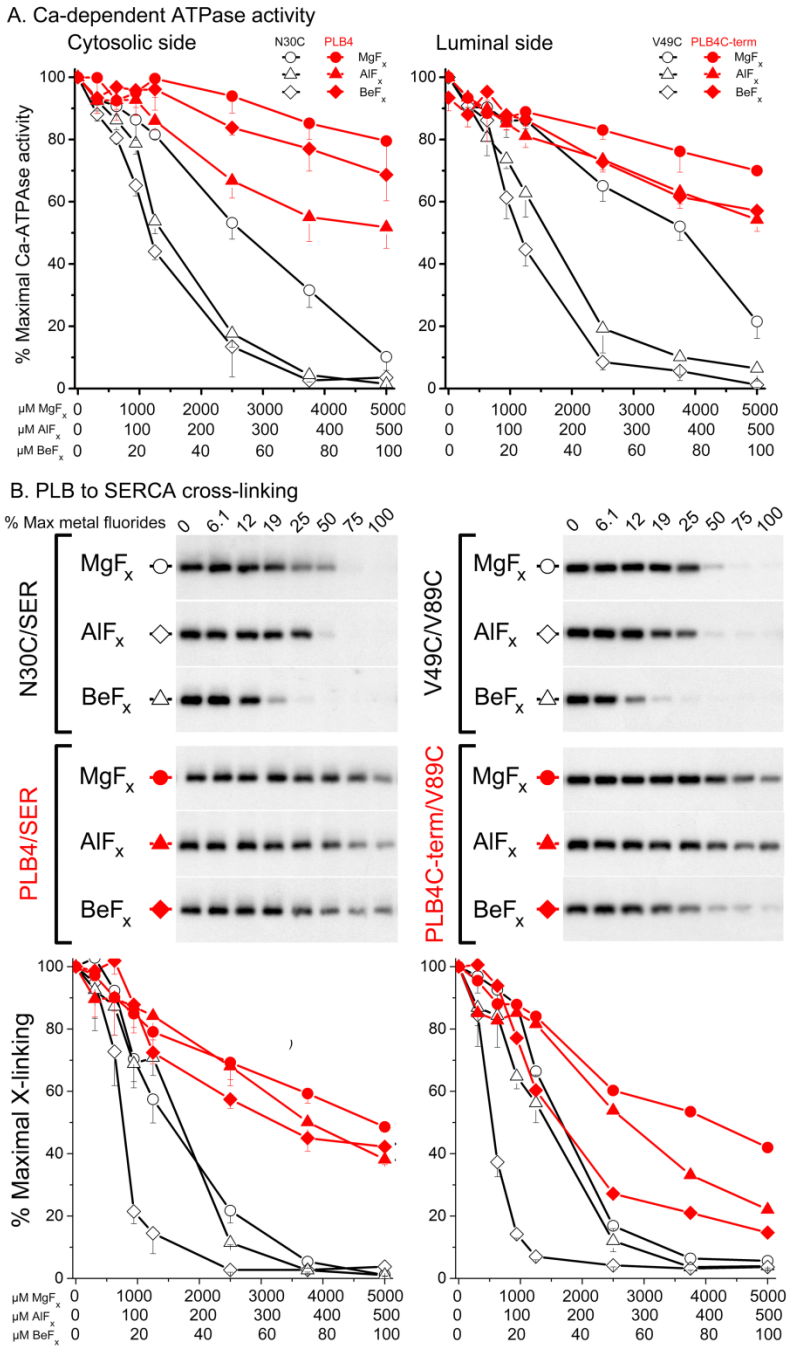
A. Ca-dependent ATPase activity
Cytosolic side
N30C
PLB4
MgFx
AlFx
BeFx
Luminal side
V49C
PLB4C-term
% Maximal Ca-ATPAse activity
µM MgFx
µM AlFx
µM BeFx
B. PLB to SERCA cross-linking
% Max metal fluorides
0
6.1
12
19
25
50
75
100
N30C/SER
V49C/V89C
PLB4/SER
PLB4C-term/V89C
% Maximal X-linking

FIGURE 6. **Nucleotide effect on MFs inhibition of cross-linking of PLB to SERCA2a.** SERCA2a was co-expressed with PLB mutants in insect cell microsomes and cross-linked as described in the legend to Fig. 4. Samples were pre-incubated 10 min in 1mM EGTA and in the absence (*Con*) and presence of saturating concentrations of MgF_x, AlF_x, or BeF_x, in various conditions as indicated: *-Nuc*, incubation with MFs in the absence of nucleotide; *Sequential*, incubation with MFs was followed by incubation with 3mM ADP or ATP. **A**. Bar graph shows the Ca^{2+}-dependent ATPase activity, measured at 0.8 mM Ca^{2+} and 1 mM EGTA for SERCA2a co-expressed with N30C-PLB and V49C-PLB, at 1.25 mM Ca^{2+} and 1 mM EGTA for SERCA2a co-expressed with PLB4, or at 1.1 mM Ca^{2+} and 1 mM EGTA for V89C-SERCA2a co-expressed with PLB4C-term. **B**. Cross-linking of normal and super-inhibitory strength PLB to SERCA2a. Each panel shows representative immunoblots of cross-linking for each PLB mutant and bar graph of MFs inhibition of cross-linking for each mutant on a percentage basis (n = 4- 6 for each mutant). The percent of maximal activity (determined in the absence of MFs and in the presence of 3mM ATP) was calculated at each condition for each PLB mutant.

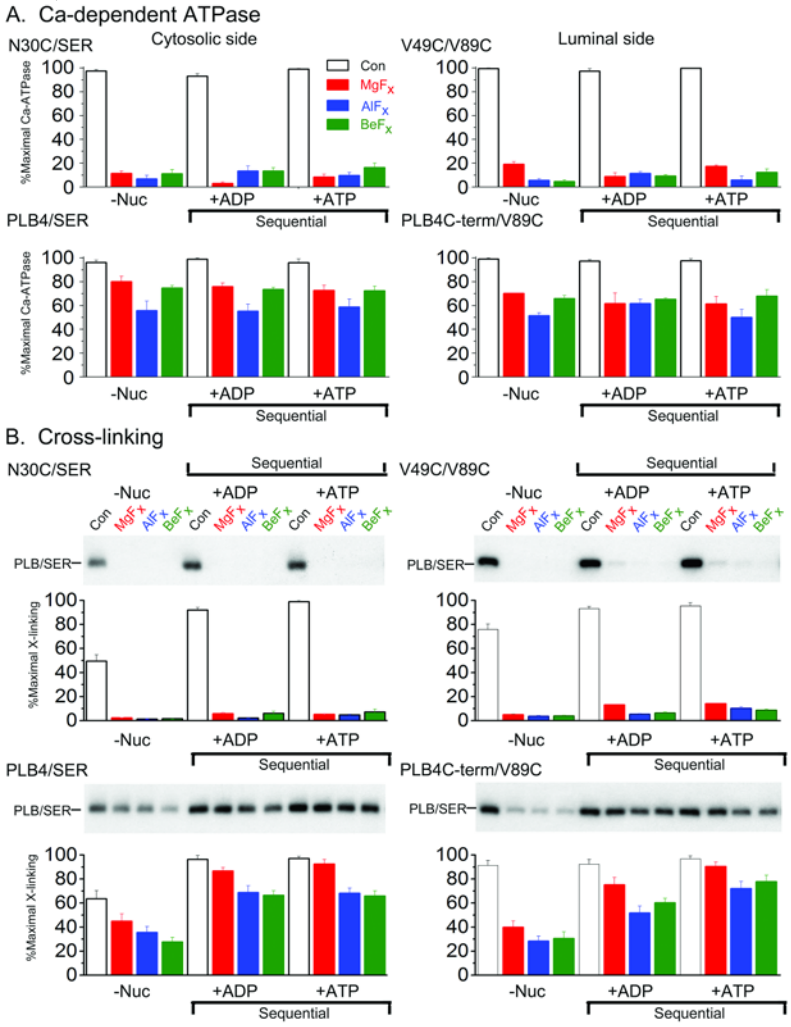

FIGURE 7. **MFs effects on ATP stimulation of PLB to SERCA2a cross-linking.** SERCA2a was co-expressed with PLB mutants in insect cell microsomes and cross-linked as described in the legend to Fig. 4. Representative immunoblots show cross-linking for each PLB mutant to SERCA2a after 10 min incubation in the presence of MFs and a series concentration of ATP as indicated at the *top*. Plots show MFs inhibition of ATP-stimulation of cross-linking for each mutant on a percentage basis (n = 4- 6 for each mutant). See Table 4 for K_{ATP} values.